INTERNATIONAL JOURNAL FOR NUMERICAL METHODS IN FLUIDS, VOL. 1, 45–61 (1981)

PERIODIC FINITE ELEMENTS IN TWO-LAYER TIDAL FLOW

MUTSUTO KAWAHARA

Department of Civil Engineering, Chuo University, Kasuga 1-Chome 13, Bunkyo-ku, Tokyo, Japan

MICHIO MORIHIRA

The First District Port Construction Bureau, Ministry of Transport, Japan

SHINJI KATAOKA

The First District Port Construction Bureau, Ministry of Transport, Japan

KEN'ICHI HASEGAWA

Port and Harbour Research Division, Unic Corporation, Japan

SUMMARY

The aim of this paper is to present the finite element method and its application to quasi-steady periodic two-layer tidal flow in estuaries and coastal seas. Formulating the weighted residual equations, using quadratic polynomials for velocity and linear polynomials for water elevation as interpolation functions and employing the periodic Galerkin method, the nonlinear simultaneous equations can be derived. The present method is used for the simulation analysis of the Niigata Port redevelopment planning.

KEY WORDS Two Layer Flow Periodic Galerkin Method Mixed Interpolation Niigata Port

INTRODUCTION

There are a number of ports located in estuaries along the coast of the Sea of Japan. In these estuaries, salt water intrudes into the river so that the patterns of current flow, sediment transport, pollutant dispersal, etc., are considerably altered. The tidal rises in almost all estuaries along the coast are so small that they are classified into a fully stratified estuary, i.e. the mixing between salt water and fresh water is incomplete. Considering this, the flow can be assumed as a two-layer, salt-water and fresh-water stratified flow.

Recently, a number of finite element methods have been presented to analyse the shallow water equation. The analyses may be classified into three fields, i.e. steady flow,[12–14,26] quasi-steady flow,[7–11,17] and unsteady flow analyses.[1–6,16,18,25] Consider the tidal motion—the flow patterns are unsteady but periodic. The unsteady flow analysis can be applied to the tidal flow analysis but results in time-consuming computation. Therefore, the quasi-steady flow analysis is necessary, provided that the flow pattern is periodic. The periodic tidal flow analysis has been dealt with by several investigators. Kawahara and Kaneko[7,8] presented the finite element method of the Navier–Stokes equation using the stream function. Kawahara and Hasegawa[9] have discussed one-layer shallow water equations employing the periodic Galerkin method. The basic idea of the method is the Fourier analysis postulating the solution as sinusoidal function series. A similar method has been used by Peason and Winter,[17] ignoring the eddy viscosity terms. Kawahara *et al.*[10] have also presented the finite element method based on the perturbation technique and sinusoidal solution.

0271–2091/81/010045–17$01.00 *Received 11 March 1980*

This paper is intended to provide the finite element method and its application to the quasi-steady periodic two-layer tidal flow in estuaries and coastal seas.[11] The method of solution is the periodic Galerkin method.[9] The application of the conventional finite element method in spatial variables leads to the finite element governing equation continuous in time. Assume that the current velocity and water elevation can be obtained by the sum of steady and periodic constituents. The Galerkin approach is employed as the numerical integration procedure in time, using the trigonometric function series as the trial function.

The present method has been applied to the development planning analysis of the Niigata Port in Japan. The port is located 250 km north of Tokyo and in the estuary of the Shinano River. The flow in the estuary is classified as a fully stratified flow. Therefore, the two-layer flow analysis is indispensable. To protect the port from the sedimentation of the sand conveyed by the river stream, a central groin has been constructed in the middle of the river. The development master plan consists of three parts: (1) removal of the central groin, (2) reclamation for a boat pier and (3) dredging of the navigation channel. The simulation study is necessary to predict the safety of ships, water quality and water usage. Before the simulation study, the field measurements were carried out to obtain the current velocity, alternation of water elevation, salt-water intrusion and water quality. By using the finite element method, one-layer and two-layer steady and periodic flow analyses have been obtained. Several useful suggestions have been made on the redevelopment planning.

BASIC EQUATIONS

The shallow water wave theory is commonly applied to represent the motion of the two-layer density flow. Consider a two-layer flow in which, for example, the upper layer is fresh water and the lower layer is salt water in an estuary. The basic equations can be derived from the three-dimensional Navier–Stokes equation under the several shallow water assumptions. Here and henceforth indicial notation and the usual summation convention with repeated indices will be employed. Let x_i be co-ordinate x and y and notation $(\ )_{,i}$ be differentiation with respect to co-ordinate x_i. The shallow water equations for the upper and lower layers can be written in the following forms, referring to Figure 1:

in the upper layer,

$$\dot{s} + \dot{d} + \{(s+d)u_i\}_{,i} = 0 \tag{1}$$

$$u_i + u_j u_{i,j} + g s_{,i} - \frac{1}{(s+d)}[A^u(s+d)(u_{i,j}+u_{j,i})]_{,j} + \gamma_{ij}u_j + \alpha_m(u_i - v_i) = 0 \tag{2}$$

and in the lower layer,

$$\dot{d} + \{(d-b)v_i\}_{,i} = 0 \tag{3}$$

$$\dot{v}_i + v_j v_{i,j} + g\{\varepsilon s_{,i} + (1-\varepsilon)d_{,i}\} + \gamma_{ij}v_j - \frac{1}{(b-d)}[A^l(b-d)(v_{i,j}+v_{j,i})]_{,j} - \beta_m(u_i - v_i) + \gamma_m v_i = 0 \tag{4}$$

where u_i and v_i denote the upper and lower velocity, respectively, and s and d represent surface and interface water elevation, respectively. Coriolis parameter means

$$\gamma_{ij} = \begin{cases} -f(i=1, j=2) \\ f(i=2, j=1) \end{cases} \quad \text{otherwise zero} \tag{5}$$

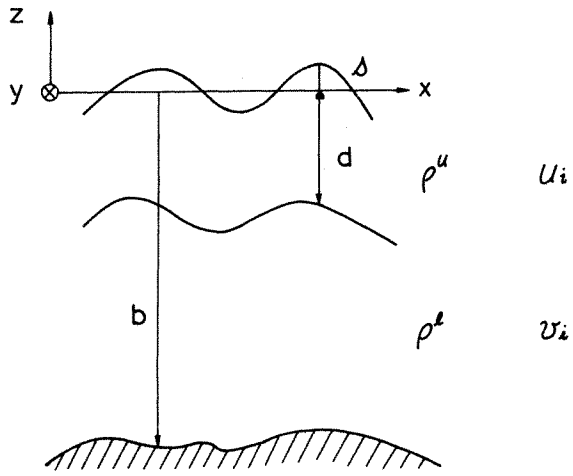

Figure 1. Co-ordinate system

and density ratio is

$$\varepsilon = \frac{\rho^u}{\rho^l} \tag{6}$$

where ρ^u and ρ^l are water density in the upper and lower layers, respectively.

Friction stresses are linearized and parameters are expressed in the following form:

$$\left.\begin{aligned} \alpha_m &= \frac{f_m}{(s+d)\rho^u} \cdot \sqrt{[(\tilde{u}_1-\tilde{v}_1)^2+(\tilde{u}_2-\tilde{v}_2)^2]} \\ \beta_m &= \frac{f_m}{(b-d)\rho^l} \cdot \sqrt{[(\tilde{u}_1-\tilde{v}_1)^2+(\tilde{u}_2-\tilde{v}_2)^2]} \\ \gamma_m &= \frac{f_b}{(b-d)\rho^l} \cdot \sqrt{(\tilde{v}_1^2+\tilde{v}_2^2)} \end{aligned}\right\} \tag{7}$$

where $\tilde{u}_i$ and $\tilde{v}_i$ express the magnitude of the upper and lower velocities, respectively, and are assumed as known constants. Friction coefficients at the interface and at the bottom of the estuary are f_m and f_b, respectively. Eddy viscosities in the upper and lower layer are represented by A^l and A^u, respectively, and gravity acceleration is g. A superposed dot ($\dot{}$) denotes the differentiation with respect to time and δ_{ij} is Kronecker's delta function.

Regarding the boundary conditions, the following are introduced. On the upper layer boundary S^u,

$$u_i = \hat{u}_i \qquad \text{on } S_1^u \tag{8}$$

$$q_i = \{-gs\delta_{ij} + A^u(u_{i,j}+u_{j,i})\}n_j = \hat{q}_i \qquad \text{on } S_2^u \tag{9}$$

$$s = \hat{s} \qquad \text{on } S_3^u \tag{10}$$

where n_j is the unit normal to the boundary surface and a superposed circumflex ($\hat{}$) denotes the prescribed value on the boundary. On the lower layer boundary S^l, similar conditions are imposed.

For the BOD concentrations C^u and C^l in the upper and lower layers, the following basic equations are employed:

in the upper layer,

$$\frac{\partial}{\partial t}(C^u h^u)+(u_j C^u h^u)_{,j}-k_{ij}(C^u h^u)_{,ij}+k(C^u-C^l)=0 \tag{11}$$

in the lower layer,

$$\frac{\partial}{\partial t}(C^l h^l)+(v_j C^l h^l)_{,j}-k_{ij}(C^l h^l)_{,ij}-k(C^u-C^l)=0 \tag{12}$$

where h^u and h^l are the thicknesses of the upper and lower layer, and k_{ij} and k are dispersion coefficients and exchange coefficients, respectively.

FINITE ELEMENT FORMULATION

Assume that the flow field of interest is divided into small regions called finite elements. The conventional finite element solution procedure leads to the global finite element equations as follows:

$$A_{\lambda\mu}(\dot{s}_\mu+\dot{d}_\mu)+D_{\lambda\mu\beta}(s_\mu+d_\mu)u_\beta=0 \tag{13}$$

$$M_{\alpha\beta}\dot{u}_\beta+K_{\alpha\beta\gamma}u_\beta u_\gamma+H_{\alpha\lambda}s_\lambda+A^u.\,S_{\alpha\beta}u_\beta+\alpha M_{\alpha\beta}(u_\beta-v_\beta)=0 \tag{14}$$

$$A_{\lambda\mu}\dot{d}_\mu+D_{\lambda\mu\beta}(d_\mu-b_\mu)v_\beta=0 \tag{15}$$

$$M_{\alpha\beta}\dot{v}_\beta+K_{\alpha\beta\gamma}v_\beta v_\gamma+H_{\alpha\lambda}\{\varepsilon s_\lambda+(1-\varepsilon)d_\lambda\}+A^l.\,S_{\alpha\beta}v_\beta-\beta M_{\alpha\beta}(u_\beta-v_\beta)+\gamma M_{\alpha\beta}v_\beta=0 \tag{16}$$

where s_λ, d_λ, u_β, v_β denote surface water elevation, interface water elevation, upper velocity and lower velocity at all nodal points in the flow field. The bottom elevation is expressed by b_λ. Coefficients in equations (13)–(16) are precisely derived in Reference 15.

The solution procedures to solve nonlinear differential equation system (13)–(16) consist of two stages. Assuming that the density difference between the upper and lower layers is ignored, the two-layer equation system reduces to the one-layer equation system. Namely, the two-layer equations can be solved by the alternative substitution of the solutions of the upper and lower layer solutions. The second stage is to solve the one-layer equation system considering periodicity.

The finite element equation system (13)–(16) can be rewritten in the following forms:

$$g_\lambda\equiv A_{\lambda\mu}\dot{Z}_\mu-D_{\lambda\mu\beta}(Z_\mu+H_\mu)U_\beta-G_\lambda=0 \tag{17}$$

$$f_\alpha\equiv M_{\alpha\beta}\dot{U}_\beta+K_{\alpha\beta\gamma}U_\beta U_\gamma+f_1H_{\alpha\lambda}Z_\lambda+A^h.\,S_{\alpha\beta}U_\beta+f_2M_{\alpha\beta}U_\beta-F_\alpha=0 \tag{18}$$

where in the case of the initial one-layer equations:

$$U_\beta=u_\beta,\qquad Z_\lambda=s_\lambda,\qquad A_h=A^u,\qquad f_1=1,$$
$$f_2=\gamma,\qquad H_\mu=-b_\mu,\qquad F_\alpha=0,\qquad G_\lambda=0$$

in the case of the lower layer equations:

$$U_\beta = v_\beta, \qquad Z_\lambda = d_\lambda, \qquad A_h = A^l, \qquad f_1 = (1-\varepsilon),$$
$$f_2 = (\beta+\gamma), \qquad H_\mu = -b_\mu, \qquad F_\alpha = \beta M_{\alpha\beta} u_\beta - \varepsilon H_{\alpha\lambda} s_\lambda,$$
$$G_\lambda = 0$$

and in the case of the upper layer equations:

$$U_\beta = u_\beta, \qquad Z_\lambda = s_\lambda, \qquad A_h = A^u, \qquad f_1 = 1,$$
$$f_2 = \alpha, \qquad H_\mu = d_\mu, \qquad F_\alpha = \alpha M_{\alpha\beta} v_\beta, \qquad G_\lambda = -A_{\lambda\mu}\dot{d}_\mu$$

Solving equations (17) and (18), the velocities and water elevations in both layers can be computed by iteration.

For the finite element method of equations (11) and (12), the conventional procedures can be successfully applied.

PERIODIC GALERKIN METHOD

To solve equations (17) and (18), the periodic Galerkin method[7-9] is employed. The method is one of the Galerkin methods applied to the integration in time, based on the fact that the motion of tidal flow is periodic. It is assumed that the given functions G_λ and F_α in equations (17) and (18) are expressed by the sum of trigonometric function series having period ω, i.e.

$$G_\lambda = G_\lambda^{(0)} + \sum_{j=1}^{N} G_{\lambda s}^{(j)} \sin(j\omega t) + \sum_{j=1}^{N} G_{\lambda c}^{(j)} \cos(j\omega t) \tag{19}$$

$$F_\alpha = F_\alpha^{(0)} + \sum_{j=1}^{N} F_{\alpha s}^{(j)} \sin(j\omega t) + \sum_{j=1}^{N} F_{\alpha c}^{(j)} \cos(j\omega t) \tag{20}$$

The weighted residual equation in time can be obtained by multiplying both sides of equations (17) and (18) by weighting functions Z_λ^* and U_α^*, respectively, and by integrating over one period:

$$\int_0^{2\pi/\omega} (Z_\lambda^* g_\lambda)\, dt = 0 \tag{21}$$

$$\int_0^{2\pi/\omega} (U_\alpha^* f_\alpha)\, dt = 0 \tag{22}$$

The trial functions are assumed to be given by

$$Z_\lambda = Z_\lambda^{(0)} + \sum_{j=1}^{N} a_\lambda^{(j)} \sin(j\omega t) + \sum_{j=1}^{N} b_\lambda^{(j)} \cos(j\omega t) \tag{23}$$

$$U_\alpha = U_\alpha^{(0)} + \sum_{j=1}^{N} c_\alpha^{(j)} \sin(j\omega t) + \sum_{j=1}^{N} d_\alpha^{(j)} \cos(j\omega t) \tag{24}$$

where $Z_\lambda^{(0)}$, $a_\lambda^{(1)} \ldots a_\lambda^{(N)}$, $b_\lambda^{(1)} \ldots b_\lambda^{(N)}$, $U_\alpha^{(0)}$, $c_\alpha^{(1)} \ldots c_\alpha^{(N)}$, $d_\alpha^{(1)} \ldots d_\alpha^{(N)}$ are the unknown vectors to be determined. The weighting function is also assumed to be expressed by the following forms:

$$Z_\lambda^* = Z_\lambda^{*(0)} + \sum_{i=1}^{N} a_\lambda^{*(i)} \sin(i\omega t) + \sum_{i=1}^{N} b_\lambda^{*(i)} \cos(i\omega t) \tag{25}$$

$$U_\alpha^* = U_\alpha^{*(0)} + \sum_{i=1}^{N} c_\alpha^{*(i)} \sin(i\omega t) + \sum_{i=1}^{N} d_\alpha^{*(i)} \cos(i\omega t) \tag{26}$$

where $Z_\lambda^{*(0)}$, $a_\lambda^{*(1)} \ldots a_\lambda^{*(N)}$, $U_\alpha^{*(0)}$, $c_\alpha^{*(1)} \ldots c_\alpha^{*(N)}$, $d_\alpha^{*(1)} \ldots d_\alpha^{*(N)}$ are the arbitrary weighting vectors. Substituting equations (23)–(26) into equations (21) and (22), rearranging the terms and using the arbitrariness of the weighting vectors, the weighted residual equations can be obtained as follows:

$$\int_0^{2\pi/\omega} g_\lambda(U_\beta^{(0)}, Z_\mu^{(0)})\,dt = 0 \tag{27}$$

$$\int_0^{2\pi/\omega} f_\alpha(U_\beta^{(0)}, Z_\mu^{(0)})\,dt = 0 \tag{28}$$

$$\int_0^{2\pi/\omega} \cos(i\omega t) g_\lambda(\omega)\,dt = 0 \tag{29}$$

$$\int_0^{2\pi/\omega} \sin(i\omega t) g_\lambda(\omega)\,dt = 0 \tag{30}$$

$$\int_0^{2\pi/\omega} \cos(i\omega t) f_\alpha(\omega)\,dt = 0 \tag{31}$$

$$\int_0^{2\pi/\omega} \sin(i\omega t) f_\alpha(\omega)\,dt = 0 \tag{32}$$

Introducing equations (23) and (24) into equations (27)–(32), the discretized nonlinear simultaneous equation system for $i = 1, 2, \ldots, N$ can be derived. The resulting steady-state equations (27) and (28) are expressed by the equations in terms of the higher order field variables. In the practical problems of the tidal flow, such as at the Niigata Port site, the coupling effect is negligibly small. For the maximum number of wave number N, it is good enough to use $N = 2$ or 3 in the case of long waves such as a tidal wave. The interpolation functions employed were the quadratic polynomial for velocity and the linear polynomial for water elevation. The precise form of the solution procedure is written in Reference 9.

APPLICATION TO THE NIIGATA PORT REDEVELOPMENT PLANNING

Niigata City is one of the leading cities in the region along the coast of the Sea of Japan. Niigata Port is the main port of the city and is located in the estuary of the Shinano River. The present investigation was carried out as the fundamental study for the development planning of the Niigata Port region. The master plan mainly consists of two parts—one is the discharge adjustment of the Shinano River by the sluice gate which will be constructed 7 km upstream, and the other is the redevelopment plan of Niigata Port itself, i.e. (1) removal of the central groin, (2) reclamation of Bandai Wharf, and (3) dredging of the navigation channel.

The central groin, indicated by A—B in Figure 2, was constructed for the purpose of separating the port from the river to protect the port from sedimentation. The construction of the sluice gate will decrease the sand conveyed by the river. For the convenience of the navigation of large-scale ships, it would be better to remove the groin. On the reclamation of the Bandai Wharf (B), a new pier for a 10,000 gross ton ferry boat will be constructed. Accordingly, the navigation channel will be dredged, of which the maximum depth will be 13 m deep.

Due to the reclamation of the Bandai Wharf, the width of the river will be 170 m wide.

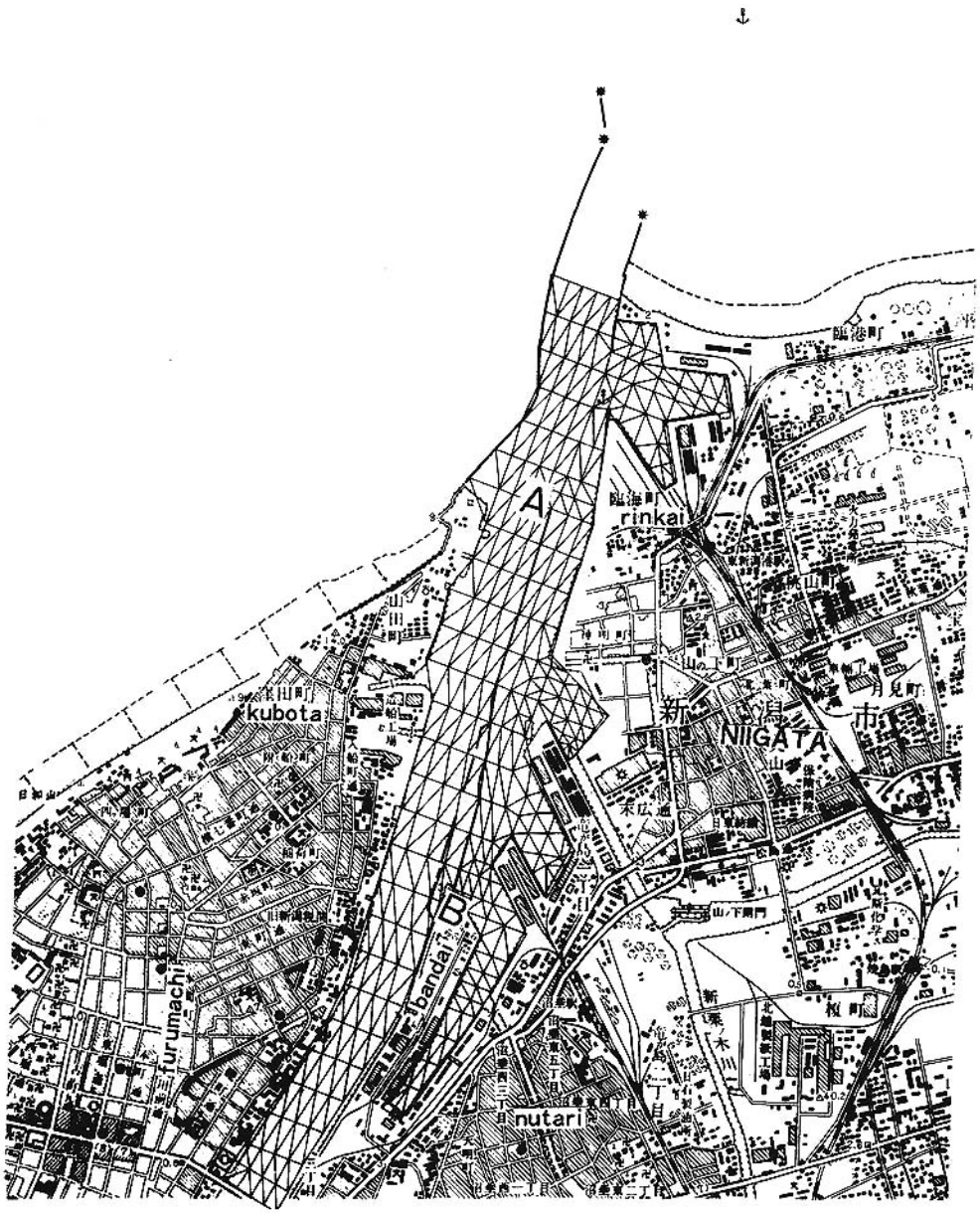

Figure 2. Analysed area at the Niigata Port

The discharge of the river will be 300 m^3/sec. The maximum velocity of the river is required to be less than 1·5 knots (≈0·75 m/sec) for the safety of ships. Water quality is regulated by the governmental laws of Niigata City. Water quality in the river was preserved well enough because the central groin protected the water in the river from the water in the port. An intake system of industrial water supply was constructed at 5 km upstream. Salt water should not reach as far as the intake.

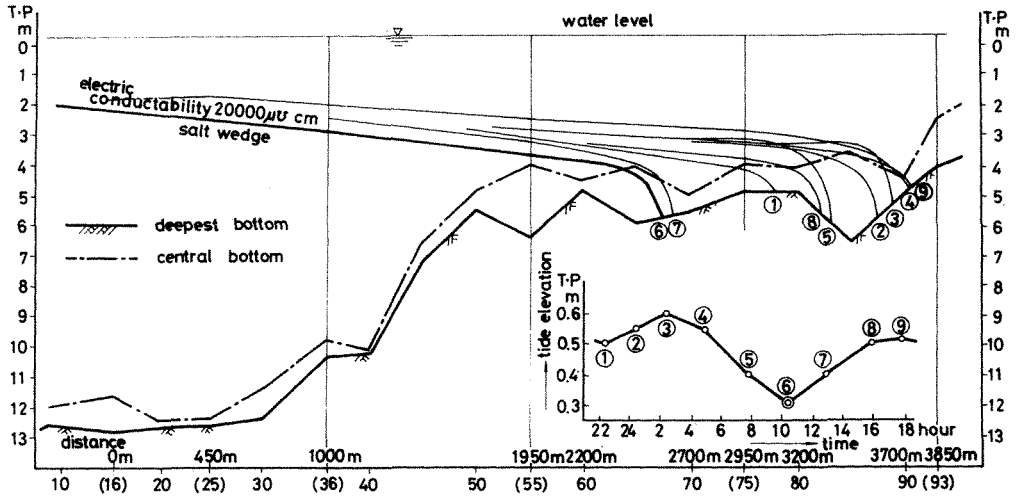

Figure 3. Observed data of the Niigata Port

Before the simulation study was carried out, field measurement was performed to ascertain the present conditions. Electric conductivity observation showed that a salt-wedge intrudes into the river as long as 3·5 km on average. The end of salt-wedge is still alternating according to the tide in the sea. Tidal water elevation difference is small in this river; the maximum difference between the high and low tide elevation is about 30 cm (Figure 3).

The maximum velocity in the fresh-water layer observed is about 80 cm/sec. On the other hand, velocity in the salt-wedge seems to be almost zero. The existing river discharge is about 400 m^3/sec and will be adjusted to be 300 m^3/sec in future by means of the construction of a sluice gate. Concerning water quality, BOD observation data is 1·0–4·6 p.p.m. on average. The average upper layer data is 2·2 p.p.m. and the lower layer is 1·2 p.p.m. The upper river water data show higher values than the lower salt-water data. This is because (1) sewage water is discharged to the upper layer water and (2) the lower layer water exchanges well with the sea water.

Figure 4 shows the finite element idealization. Total numbers of finite elements and nodal points are 555 and 368 per each layer, respectively. Concerning one-layer analysis, the

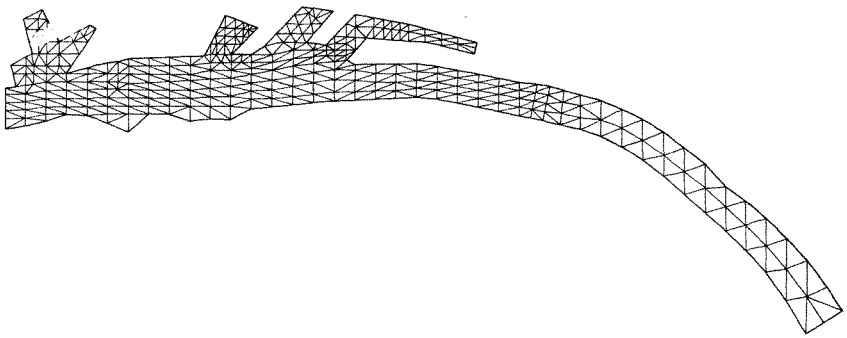

Figure 4. Finite element idealization

following assumptions are used. The observed upper fresh-water depth is assumed and the parabolic profile of the river velocity is specified on the upstream boundary. On both sides of the river, the no-slip boundary condition is used. On the downstream boundary, the open ocean boundary condition, i.e. the traction force of the boundary is zero, is imposed. As the eddy viscosity, 10^5 cm/sec is used, after several numerical trials. Concerning two-layer analysis, the following assumptions are also employed. As the interface elevation, the observed mean water elevation is used. On the open ocean boundary, tidal water elevation $M_2+S_2=8{\cdot}7$ cm is imposed for the surface and interface water elevation.

The interfacial friction coefficient f_m is assumed as the function of the internal Reynolds number and the internal Froud number and it was calibrated by several trial computations. Concerning the water quality analysis, the diffusion coefficient is assumed to be 5×10^5 cm^2/sec, and the BOD value at the ocean boundary is specified as 1 p.p.m. Exchange coefficient of the contaminant between the upper and lower layer is assumed to be $1{\cdot}3\times10^{-3}$ cm/sec.

SIMULATION RESULTS

The observed data shows that, in the upper layer flow, the river current is dominant and, on the other hand, in the lower layer flow, the tidal current is evident but its absolute value is small. Considering this, for the computation of the drift current, a one-layer analysis was carried out using the observed upper layer depth. For the computation of the lower current, a two-layer analysis was performed, considering tidal periodicity. Comparative computations were obtained for the current velocity, (1) with the central groin, (2) half removal of the central groin, and (3) without the central groin, using the corresponding port configurations of the reclamation.

In the case of one-layer flow analysis, the computed current velocities are shown in Figures 5 and 6. Specifying the upstream discharge of the river as 400 m^3/sec, the current velocity is computed and is represented in Figure 5. Maximum velocity for the cross-section at the river mouth is 0·76 m/sec, and 0·56 m/sec in the middle part of the river. The observed current velocity is about the same order as of the completed results. It is seen that the central groin completely separates the water in the port from the one in the river. The computed velocity is shown in Figure 6, specifying the upstream discharge as 300 m^3/sec and using the corresponding future configurations. The maximum velocities at the same section will vary at 0·48 m/sec, 0·93 m/sec and 0·79 m/sec, respectively. This is because the river flow depends both on the width of the river and depth of the water. The current in the port near the wharf is not severely affected by the removal of the central groin. The average velocity is about 3–4 cm/sec.

In the case of two-layer flow analysis, the computed results are shown in Figures 7–9. From the computed results, the following conclusions are obtained. The upper layer current velocity is not affected by the tidal motion, i.e. the computed velocity is almost the same as that in the one-layer flow analysis. The length of the salt-water wedge in the lower layer will shorten according to the increase in river discharge. The salt-water wedge without the central groin will be 1·8–2 times longer than that of the existing river. The lower current velocity is not affected by the removal of the central wall.

In the case of water quality analysis, the computed BOD concentration is shown in Figures 10 and 11. In the computation of one-layer dispersion analysis, the concentration computed shows much higher values than that of the observed data. On the contrary, by two-layer dispersion analysis, the numerical results computed close to the observed data can be

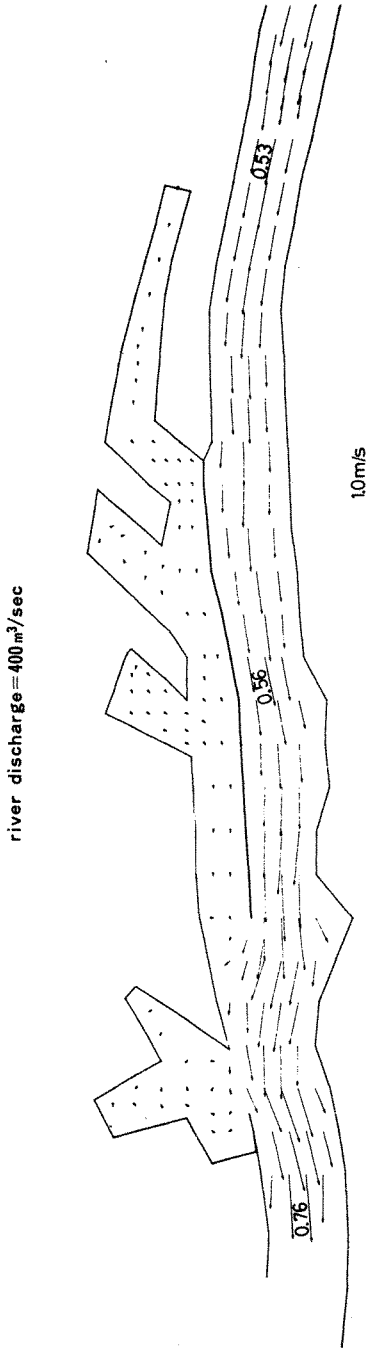

Figure 5. Computed velocity using one-layer model

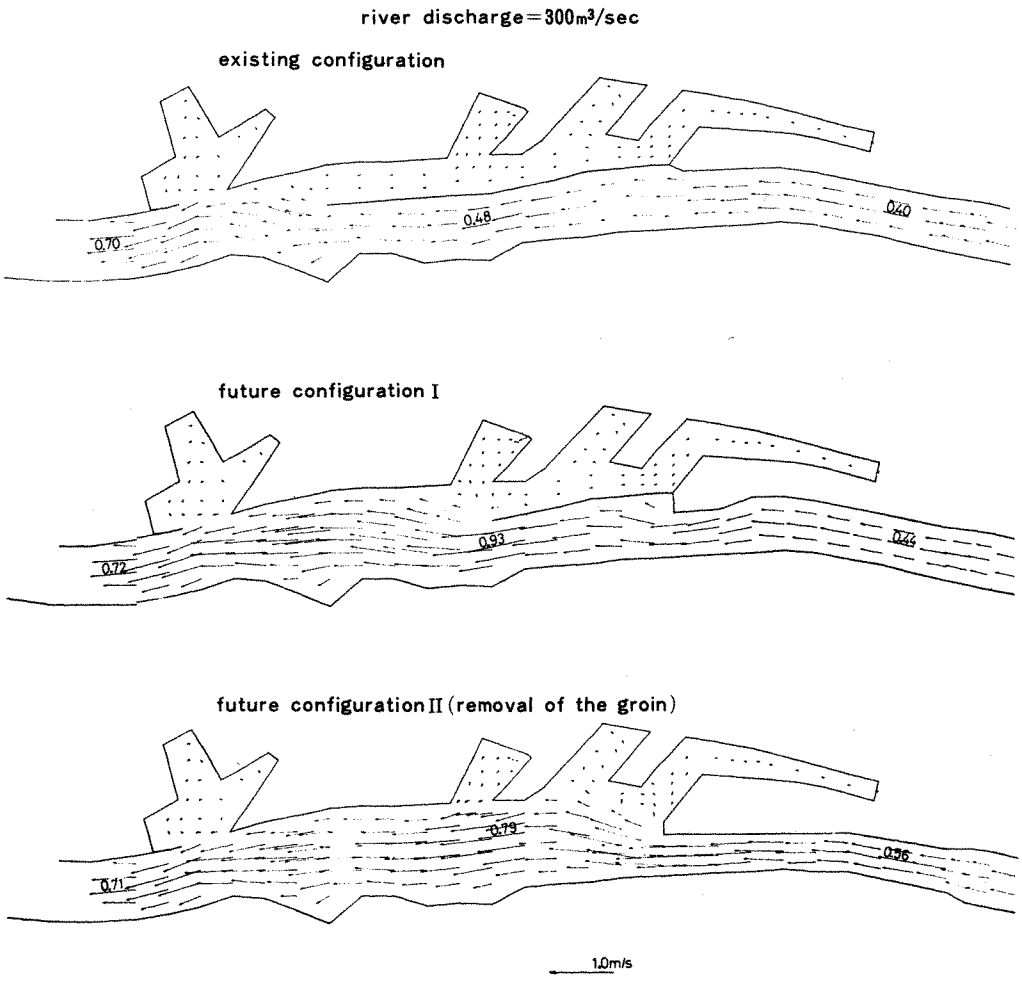

Figure 6. Comparison of computed velocity

obtained. Therefore, it is seen that the contaminant transport is carried out, including the exchange of the upper and lower layer. Using the existing configuration, the maximum BOD concentration is computed up to 10–11 p.p.m. and the average is about 5 p.p.m. By removal of the central groin, water quality will be improved because water exchange with the sea will be accelerated. The sewage discharge will decrease by the development of the sewage system. Therefore, the maximum BOD concentration computed in the future is 6 p.p.m. and the average value is less than 2·5 p.p.m. The concentration in the lower layer will be 1·2–1·8 p.p.m.

For the simulation results, the following conclusions can be derived:

1. By removal of the central wall, the width of the river will be wider than at present. However, salt water will readily intrude into the river and reach further upstream. Therefore, since the cross-section of the upper layer will be almost the same, in total, the maximum velocity of the river will not alter.

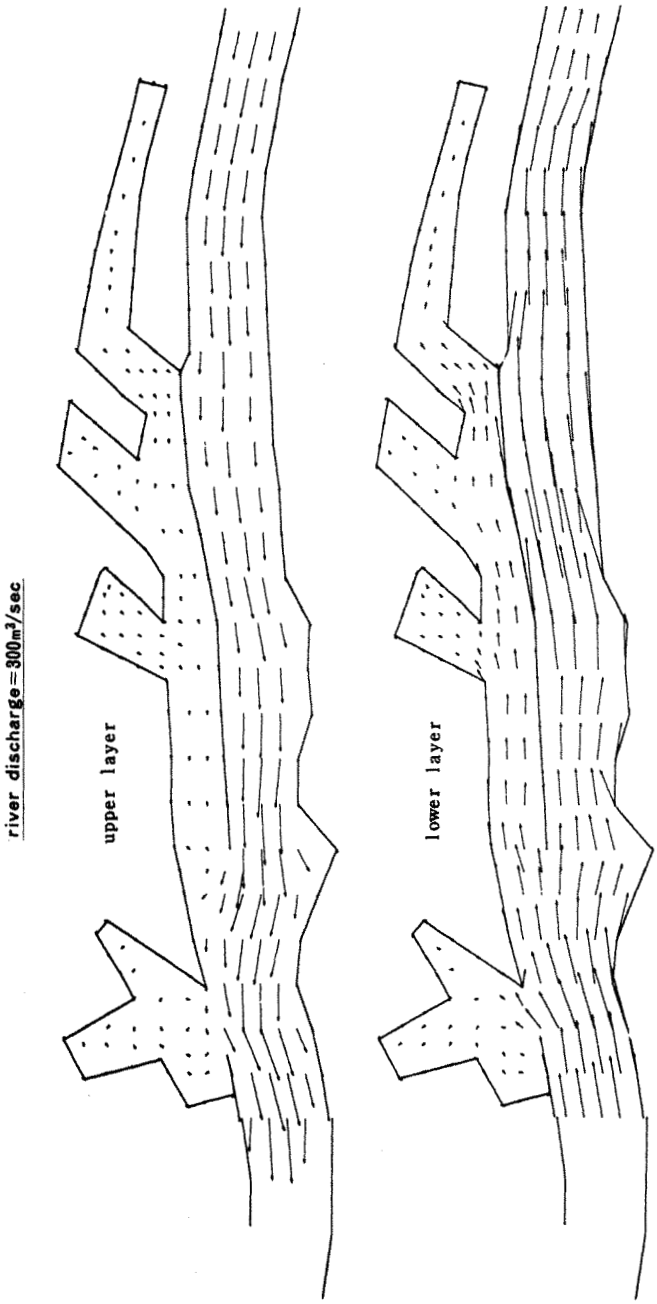

Figure 7. Computed velocity using two-layer model with existing configuration

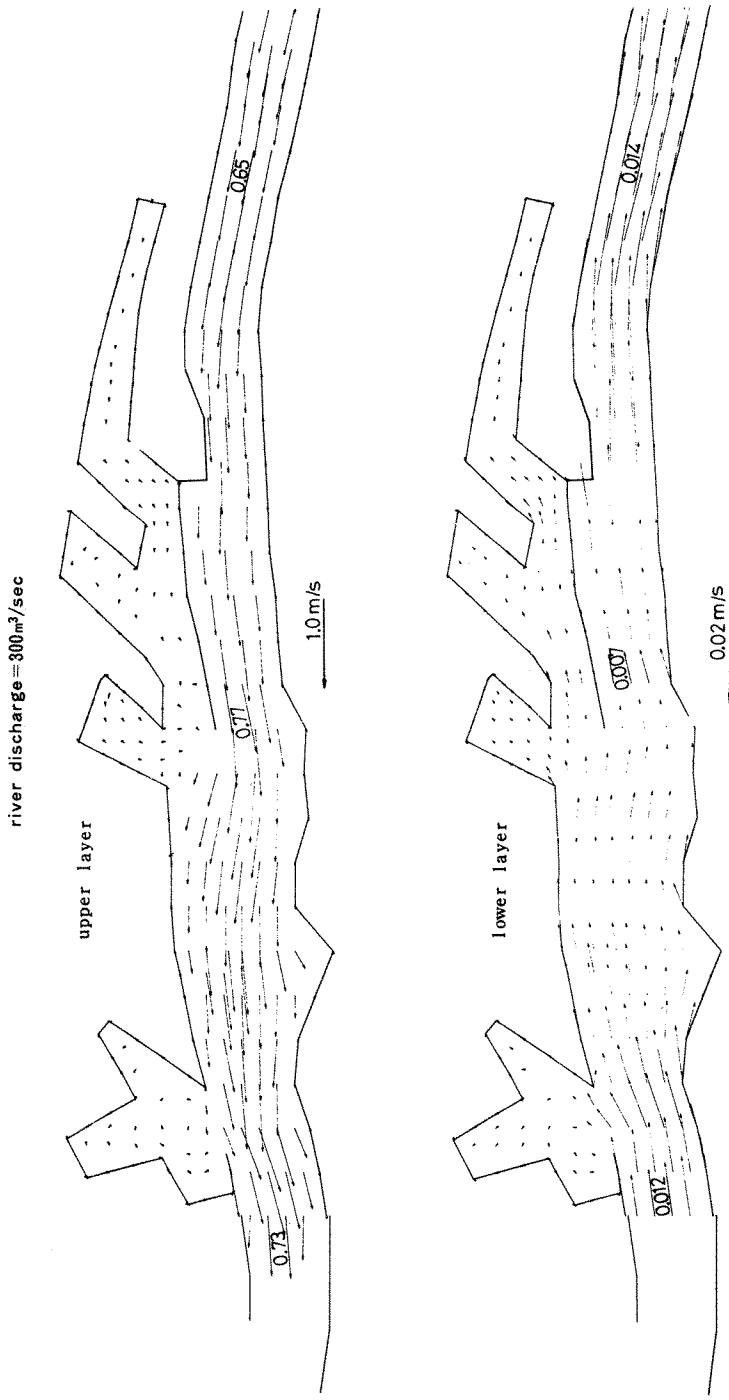

Figure 8. Computed velocity using two-layer model with future configuration I

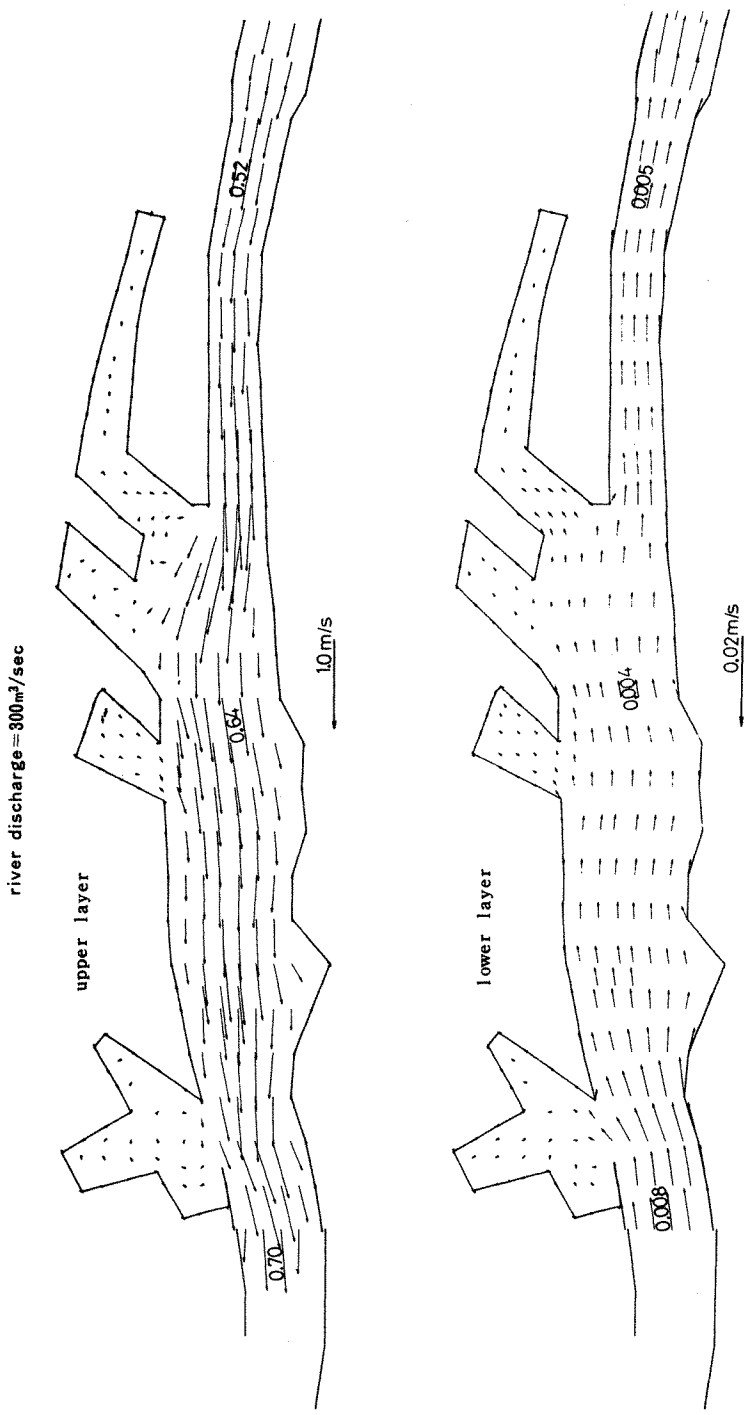

Figure 9. Computed velocity using two-layer model with future configuration II

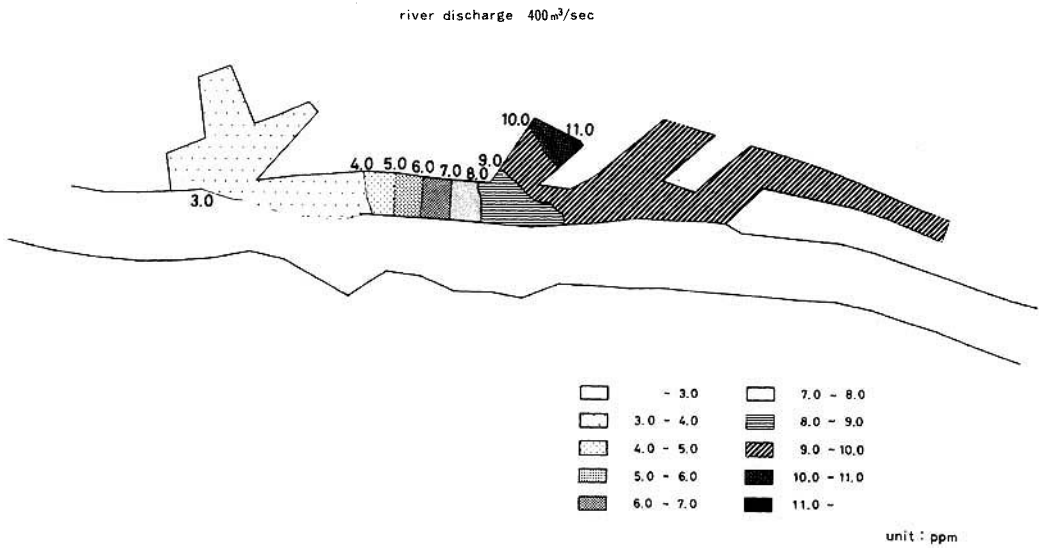

Figure 10. Computed contaminant distribution with existing configuration

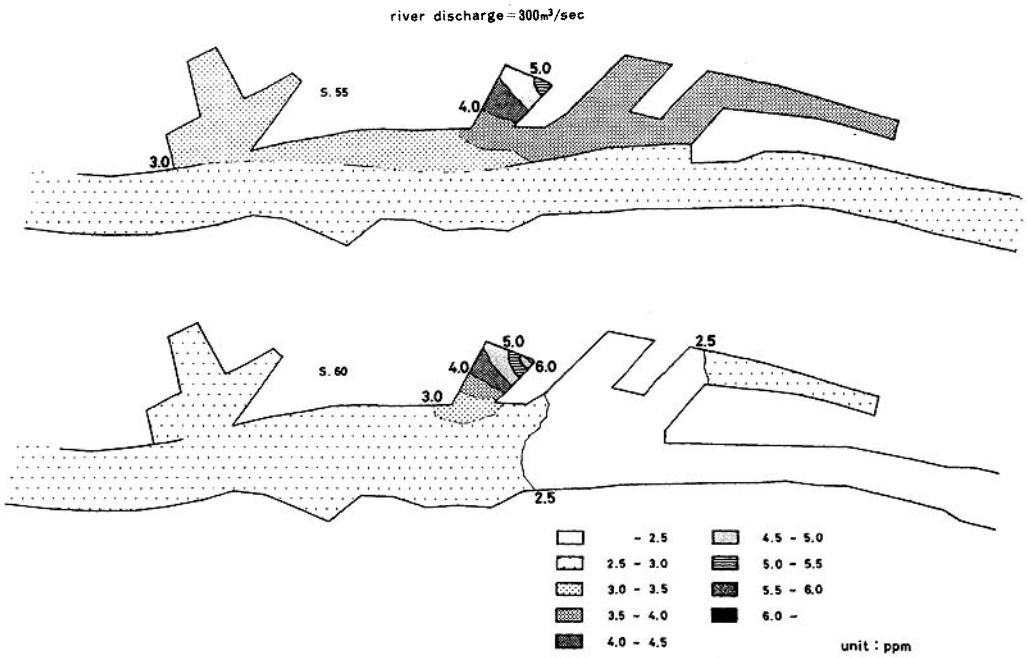

Figure 11. Computed contaminant distribution with future configuration II

2. By reclamation of the Bandai Wharf, the width of the river will be narrowed. The velocity at the channel will be 1·8–2·0 times the present velocity.
3. By removal of the central wall, the water quality of the port will be improved to be the same quality as of the main river.
4. Design discharge from the sluice gate which will be constructed is decided to be 300 m^3/sec, considering the navigation, the water resources and the water quality.

CONCLUSION

The finite element method has been applied to the two-layer flow analysis, postulating that the flow is periodic. The present method is used for the simulation analysis of the Niigata Port redevelopment planning. Using the finite element method, the configuration of the coastal boundary and bottom topography of the sea can be flexibly approximated by the triangular elements. Thus, the method is suitable for the simulation analysis such as before and after studies concerned with the construction of sea structures. To reduce the computation time, the present method has employed the Galerkin technique in time, using the sinusoidal function solution. The present numerical procedure was shown to be suitable and of practical use in the analysis of the two-layer flow problem from the viewpoint computation time, computational core storage and numerical stability.

REFERENCES

1. C. A. Brebbia and P. W. Partridge, 'Finite element simulation of water circulation in the North Sea', *Appl. Math. Model.*, **1**(2), 101–107 (1976).
2. R. T. Cheng, 'Transient three-dimensional circulation of lakes', *Proc. ASCE*, **103,** (EM 1), 17–34 (1977).
3. M. J. P. Cullen, 'A simple finite element method for meteorological problems', *J. Inst. Math. Appl.*, **11,** 15–31 (1973).
4. W. G. Gray, 'An efficient finite element scheme for two dimensional surface water computation', in *Finite Elements in Water Resources* (Eds. Pinder *et al.*), Princeton University, Pentech Press, 1976, pp. 433–449.
5. K. P. Holz and H. Hennlich, 'Numerical experiences from the computation of tidal waves by the finite element method', in *Finite Elements in Water Resources* (Eds. Pinder *et al.*), Princeton University, Pentech Press, 1976, pp. 419–431.
6. J. R. Houston, 'Interaction of Tsunamis with the Hawaiian Islands calculated by a finite element model', *J. Phys. Ocean.*, **8,** 93–102 (1978).
7. M. Kawahara and N. Kaneko, 'Periodic Galerkin finite element method of incompresible viscous fluid flow', in *Theoretical and Applied Mechanics*, vol. 25, University of Tokyo Press, 1977, 329–338.
8. M. Kawahara, 'Periodic Galerkin finite element method of unsteady flow of viscous fluid', *Int. J. num. Meth. Engng*, **11**(7), 1093–1105 (1977).
9. M. Kawahara and K. Hasegawa, 'Periodic Galerkin finite element method of tidal flow', *Int. J. num. Meth. Engng*, **12,** 115–127 (1978).
10. M. Kawahara, K. Hasegawa and Y. Kawanago, 'Periodic tidal flow analysis by finite element perturbation method', *Comp. Fluid*, **5,** 175–189 (1977).
11. M. Kawahara and K. Hasegawa, 'Finite element analysis of two layered tidal flow', in *Applications of Computer Methods in Engineering* (Ed. L. C. Wellford, Jr.), University of Southern California, 1977, pp. 1357–1366.
12. M. Kawahara and T. Okamoto, 'Finite element analysis of steady flow of viscous fluid using stream function', *Proc. JSCE*, no. 247, pp. 123–135 (1976).
13. M. Kawahara, 'Steady and unsteady finite element analysis of incompressible viscous fluid', in *Finite Elements in Fluids*, vol. 3, Wiley, Chichester, 1978.
14. M. Kawahara, 'Finite element methods of drift currents in coastal seas and estuaries using stream function, *TICOM Report, No.* 78–11, University of Texas at Austin, 1978.
15. M. Kawahara, M. Morihira, S. Kataoka and K. Hasegawa, 'Periodic finite elements in two layer tidal flow', *Bull. Facul. Sci & Eng. Chuo Univ.*, **21,** 151–175 (1978).
16. P. W. Partridge and C. A. Brebbia, 'Quadratic finite elements in shallow water problems', *Proc. ASCE*, **102,** (HY9), 1299–1313 (1976).
17. C. E. Peason and D. F. Winter: 'On the calculation of tidal currents in homogeneous estuaries,' *J. Phys. Ocean.*, **7**(6), 520–531 (1977).

18. J. Sündermann, 'Computation of barotoropic tides by the finite element method', in *Finite Elements in Water Resources* (Eds. Pinder *et al.*), Princeton University, Pentech Press, 1976, pp. 4–51 to 4–67.
19. C. Taylor and J. M. Davis, 'Tidal and long wave propagation—a finite element approach', *Comp. Fluid.*, **3,** 125–148 (1975).
20. C. Taylor and J. M. Davis: 'Tidal propagation and dispersion in estuaries', in *Finite Elements in Fluids*, Wiley, 1976, pp. 95–118.
21. J. D. Wang, 'Multi-level finite element hydrodynamic model of Block Island Sound, in *Finite Elements in Water Resources* (Eds. Pinder *et al.*), Princeton University, Pentech Press, 1976 pp. 469–493.
22. J. D. Wang, 'Real time flow in unstratified shallow water flow', *Proc. ASCE*, **104** (WW1), 53–68 (1978).
23. D. L. Young, J. A. Liggett and R. H. Gallagher, 'Steady stratified circulation in a cavity', *Proc. ASCE*, **102** (EM1), 1–17 (176).
24. D. L. Young, J. A. Liggett and R. H. Gallagher, 'Unsteady stratified circulation in a cavity', *Proc. ASCE*, **102** (EM6), 1009–1023 (1976).
25. D. L. Young and J. A. Liggett: 'Transient finite element shallow lake circulation', *Proc. ASCE*, **103** (HY2), 109–121 (1977).
26. O. C. Zienkiewicz, *The Finite Element Method*, 3rd edn, McGraw-Hill, London, 1977.